Acta Crystallographica Section D
Biological Crystallography
ISSN 0907-4449

The structure of T_6 bovine insulin

G. David Smith,[a,b]* Walter A. Pangborn[b,c] and Robert H. Blessing[b,c]

[a]Structural Biology and Biochemistry, Hospital for Sick Children, 555 University Avenue, Toronto, Ontario M5G 1X8, Canada, [b]Hauptman–Woodward Medical Research Institute, 700 Ellicott Street, Buffalo, NY 14203, USA, and [c]Department of Structural Biology, School of Medicine and Biomedical Sciences, State University of New York at Buffalo, USA

Correspondence e-mail: gdsmith@sickkids.ca

Received 13 July 2005
Accepted 11 August 2005

PDB Reference: T_6 bovine insulin, 2a3g, r2a3gsf.

Porcine insulin differs in sequence from bovine insulin at residues A8 (Thr in porcine→Ala in bovine) and A10 (Ile in porcine→Val in bovine). The structure of T_6 hexameric bovine insulin has been determined to 2.25 Å resolution at room temperature and refined to a residual of 0.162. The structure of the independent dimer is nearly identical to the T_6 porcine insulin dimer: the mean displacement of all backbone atoms is 0.16 Å, with the largest displacements occurring at AlaB30. Each of two independent zinc ions is octahedrally coordinated by three HisB10 side chains and three water molecules. As has been observed in both human and porcine insulin, the GluB13 side chains are directed towards the center of the hexamer, where a short contact of 2.57 Å occurs between two independent carboxyl O atoms, again suggesting the presence of a centered hydrogen bond. No significant displacements of backbone atoms or changes in conformation are observed at A8 or A10. Since there are no interhexamer hydrogen-bonded contacts involving A8 in either porcine or bovine insulin, the change in the identity of this residue appears to have little or no effect upon the packing of the hexamers in the unit cell. In contrast, the side chains of the three A10 residues in one trimer make van der Waals contacts with the A10 side chains in a translationally related hexamer. As a consequence of the loss of the $C^{\delta1}$ atom from the isoleucine residue in porcine insulin to produce valine in bovine insulin, there is a 0.36 Å decrease in the distance between independent pairs of C^{β} atoms and a 0.24 Å decrease in the *c* dimension of the unit cell. Thus, the net effect of the change in sequence at A10 is to strengthen the stabilizing hydrophobic interactions between hexamers.

1. Introduction

Insulin, a polypeptide hormone critical for the metabolism of glucose, consists of a 21-residue A chain and a 30-residue B chain linked by two disulfide bonds; an additional intra-A-chain disulfide bond links CysA6 and CysA11. The A chain consists of two α-helical segments connected by an extended section of polypeptide chain, while the B chain consists of two extended segments connected by a central α-helical segment. Numerous spectroscopic (Krüger *et al.*, 1990; Choi *et al.*, 1993; Brzović *et al.*, 1994; Bloom *et al.*, 1995) and X-ray crystallographic (Derewenda *et al.*, 1989; Smith & Dodson, 1992; Ciszak & Smith, 1994; Whittingham *et al.*, 1995; Smith *et al.*, 1996, 2000, 2001) studies have shown hexameric insulin to be allosteric. In order to avoid confusion in naming the various hexameric types, the T, R and R^f nomenclature is used (Kaarsholm *et al.*, 1989; Ciszak *et al.*, 1995). The T conformation has residues B1–B8 as extended with B9–B19 α-helical, while B1–B19 are α-helical in the R conformation

and the R^f conformation is similar to R except that B1–B3 are extended. Using this nomenclature, observed insulin hexamers are named T_6, $T_3R_3^f$ and R_6.

Long-acting therapeutic forms of insulin such as Ultralente are microcrystalline suspensions of hexameric zinc insulin that provide a basal level of insulin for the control of diabetes. Ideally, the basal level should be relatively constant in order to maintain constant blood-glucose levels. These long-acting preparations are initially produced in the presence of a sodium chloride concentration of 1.2 *M* but are later diluted to 0.12 *M* (Richards *et al.*, 1999). Crystallographic studies have shown that in the presence of 0.5 *M* sodium chloride, crystals are obtained that contain $T_3R_3^f$ hexamers rather than T_6 hexamers (de Graff *et al.*, 1981). Based upon the structure of $T_3R_3^f$ human insulin, in which one of the zinc ions is buried some 13.5 Å deep in the complex and isolated from the external environment, it was suggested that long-acting therapeutic forms of insulin contained $T_3R_3^f$ hexamers (Smith *et al.*, 1984). However, recent powder diffraction results on human Ultralente insulin show that the microcrystals grown in the presence of 1.2 *M* sodium chloride are in fact $T_3R_3^f$, but that the dilution to 0.12 *M* for these therapeutic preparations induces the R→T transition, resulting in T_6 hexamers (Richards *et al.*, 1999).

Prior to the production of biosynthetic human insulin, therapeutic insulin preparations were derived from either porcine or bovine insulin. Porcine insulin differs in sequence from human insulin at B30 (human, Thr; porcine, Ala), while bovine insulin differs in sequence from porcine insulin at A8 (bovine, Ala; porcine, Thr) and A10 (bovine, Val; porcine, Ile). Although the bovine sequence difference from human or porcine insulin is relatively minor, it is sufficient to produce an immune response in some individuals. A pharmacokinetic study of human, porcine and bovine Ultralente preparations (Seigler *et al.*, 1991) showed that over a period of 30 h the plasma level of bovine insulin was relatively constant, while the plasma levels of both human and porcine insulin peaked at approximately 8–20 h following injection. Thus, from a therapeutic point of view, beef insulin has a superior pharmacodynamic profile. This could arise from a slower rate of dissolution of the microcrystals to release insulin hexamers into solution, a slower rate of dissociation of dissolved hexamers to release hormonally active insulin monomers or both.

The present study was undertaken in order to ascertain whether the differences in sequence in bovine insulin at A8 and A10 produced any minor alterations in the A-chain conformation or significantly altered the intrahexamer and interhexamer interactions in the crystal.

2. Experimental

2.1. Crystallization

Highly purified bovine insulin complexed with zinc was provided by Lilly Research Laboratories. Buffer, salts and other reagents were purchased and used without further purification. The crystallization medium contained 0.6 mg ml^{-1} bovine insulin, 0.01 *M* HCl, 0.007 *M* zinc acetate, 0.05 *M* sodium citrate and 17% acetone. The pH was raised to 8.0 to ensure complete dissolution of the bovine insulin and then reduced to 6.2. The solution was warmed to 323 K and allowed to cool to room temperature over a period of several days. The crystals were rhomboidal in shape and ranged in size from 0.2 to 0.5 mm on each edge.

Table 1
Data-measurement statistics for T_6 bovine insulin.

Space group	*R*3
Unit-cell parameters	
a (Å)	82.55
b (Å)	82.55
c (Å)	33.76
α (°)	90.0
β (°)	90.0
γ (°)	120.0
Temperature (K)	293
$\langle B_{iso}\rangle$ (Å^2)	25.9
No. of frames	36
Resolution (Å)	2.20
Total data	17545
Unique data	4345
Average redundancy	4.04
Completeness (%)	99.5
Total missing data	19
Overall R_{merge}	0.051
$\langle F^2\rangle/\langle\sigma(F^2)\rangle$	18.1
Statistics for resolution range 2.31–2.25 Å	
Completeness (%)	100.0
$F^2/\sigma(F^2) > 3$ (%)	55.2
$\langle F^2\rangle/\langle\sigma(F^2)\rangle$	4.06
R_{merge}	0.175
Statistics for resolution range 2.25–2.20 Å	
Completeness (%)	94.0
$F^2/\sigma(F^2) > 3$ (%)	40.4
$\langle F^2\rangle/\langle\sigma(F^2)\rangle$	2.81
R_{merge}	0.202

2.2. Data measurement

A well formed single crystal was mounted in a quartz capillary along with a drop of mother liquor. Data were measured at room temperature using a Rigaku R-AXIS IIC image-plate system and an RU-200 rotating-anode generator with graphite-monochomated Cu $K\alpha$ (λ = 1.54178 Å) radiation. Integration, scaling and merging of the data were performed with *DENZO* and *SCALEPACK* (Otwinowski & Minor, 1997). The independent data were processed further by *SORTAV*, *BAYES* and *LEVY* (Blessing, 1997) to reformat the data, to apply Bayesian statistics and to estimate the scale factor and overall isotropic temperature factor, respectively. Unit-cell, space-group and data-measurement statistics are given in Table 1.

2.3. Structure solution and refinement

The initial model consisted of the room-temperature structure of the T_6 porcine insulin dimer (PDB code 4ins; Baker *et al.*, 1988), from which all water molecules and alternate side chains were excluded; each atom in the starting model was assigned the unit-cell average temperature factor obtained from the Wilson analysis in *LEVY*. No reflections to a resolution of 2.25 Å were excluded from the data set.

Table 2
Data-refinement statistics for T_6 bovine insulin.

Values in parentheses are for the highest resolution shell.

Resolution range (Å)	30.5–2.25 (2.39–2.25)
No. of reflections	4069 (607)
R value	0.162 (0.204)
R_{free} value	0.219 (0.258)
Completeness in last shell (%)	100.0
Cross-validated σ_A estimated error (Å)	0.25
R.m.s. deviations from ideal	
Bond lengths (Å)	0.006
Bond angles (°)	1.08
Dihedral angles (°)	21.3
Improper angles (°)	0.70
Isotropic thermal model restraints (Å^2)	
Main-chain bonds	1.45
Main-chain angles	2.40
Side-chain bonds	2.32
Side-chain angles	3.53

Approximately 10% of the data were reserved for cross-validation (Brünger, 1992) and were not used at any point during the refinement. A single cycle of *CNS* refinement, applying an overall anisotropic temperature-factor correction, a bulk-solvent correction and using maximum-likelihood torsion-angle dynamics followed by individual temperature-factor refinement (Rice & Brünger, 1994; Pannu & Read, 1996; Adams *et al.*, 1997; Brünger *et al.*, 1998), yielded a residual of 0.214 and an R_{free} of 0.269. As the refinement continued, σ_A-weighted $2F_o - F_c$ and $F_o - F_c$ maps as implemented in *CNS* (Read, 1986; Brünger *et al.*, 1997) were carefully examined with *CHAIN* (Sack, 1988). Adjustments were made to main-chain and side-chain atoms and water molecules were added in accord with good electron density and the formation of hydrogen bonds to existing atoms within the model. The refinement was continued, including conjugate-gradient refinement in cases in which torsion-angle refinement was deemed to be unnecessary (no significant additions or changes in the protein model had been made). Bonds and angles involving the zinc ions and their ligands were not restrained. Particular attention was paid to the side chains of those residues in the T_6 porcine structure that were observed to be disordered, as well as the two residues in the bovine sequence which differ from those in the porcine sequence. The geometry was continually monitored with *PROCHECK* (Laskowski *et al.*, 1993). Near the end of the refinement, the difference electron densities in the vicinity of the side chains of residues ValA10.1[1] and ValB12.1 suggested disorder and these residues were modeled as such. At the end of the refinement, the model consisted of 796 protein atoms, two zinc ions and 56 water molecules. No electron density was observable for the side chain of GluB21.1 and it was therefore modeled as alanine. A total of 82 (95.3%) and four (4.7%) of the non-glycine or non-proline residues lie in the most favored or additional allowed regions of the Ramachandran plot, respectively, as determined by *PROCHECK* (Laskowski *et al.*, 1993); no residues lie within the generously allowed or disallowed regions. Refinement statistics are given in Table 2.

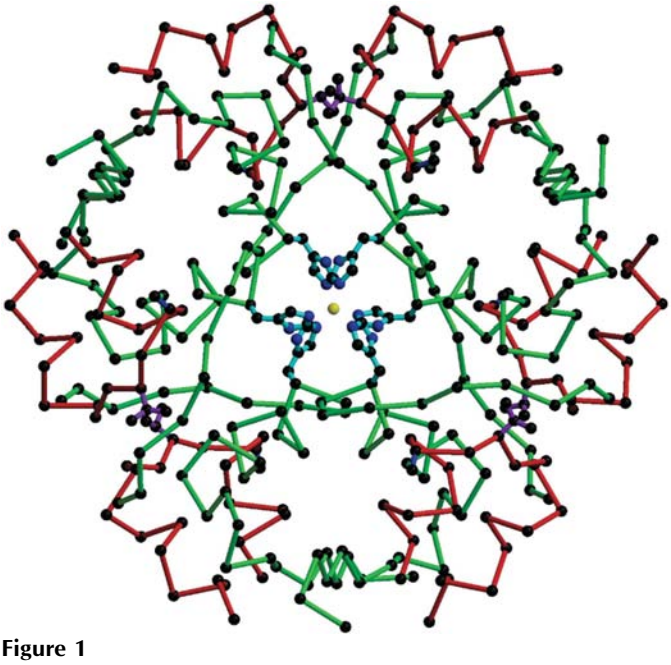

Figure 1
C^α trace of the T_6 bovine insulin hexamer as viewed down the crystallographic threefold axis. A chains are colored red, B chains green, AlaA8 blue, ValA10 purple, HisB10 cyan and zinc ions yellow. Because both zinc ions lie on the threefold axis, only one is visible in the drawing. Water molecules bound to zinc have been omitted for clarity. This figure was prepared with the programs *MOLSCRIPT* (Kraulis, 1991) and *RASTER3D* (Merritt & Bacon, 1997).

3. Results and discussion

3.1. Dimer conformations

A *MOLSCRIPT* drawing (Kraulis, 1991) of the T_6 bovine insulin hexamer is illustrated in Fig. 1. The independent T_2 bovine insulin dimer was fitted by a least-squares procedure (Smith, 1993) to the T_2 porcine insulin dimer (Baker *et al.*, 1988), minimizing all backbone atom displacements, and resulted in mean and r.m.s. displacements of 0.16 and 0.20 Å, respectively. C^α displacements are plotted for the A and B chains in Figs. 2(*a*) and 2(*b*), respectively. The largest displacement occurs at the C-terminus of the B chains, where displacements of 1.14 and 0.36 Å are observed for monomers 1 and 2, respectively. Based upon a cross-validated σ_A-estimated coordinate error of 0.25 Å (see Table 2), the mean displacement is less than the estimated error in the coordinates, which shows that with the exception of two B30 residues the bovine and porcine structures do not differ significantly. Excluding both AlaB30 residues, a total of 13 displacements at C^α exceed 0.25 Å: GlyA1.1 (0.36 Å), IleA2.1 (0.30 Å), GluA4.1 (0.29 Å), AlaA8.1 (0.26 Å), TyrA14.1 (0.27 Å), PheB1.1 (0.28 Å), GlyA1.2 (0.45 Å), GluA4.2 (0.30 Å), GlnA5.2 (0.49 Å), SerA9.2 (0.37 Å), ValA10.2 (0.26 Å), ValB2.2 (0.38 Å) and GlyB20.2 (0.28 Å). While none of these displacements is exceptional, nine of the 16 largest displacements occur within the first ten residues of the A chains, but no significantly large displacements occur at either AlaA8 or ValA10, the two

[1] The decimal portion of the residue number refers to either monomer 1 or monomer 2 of the dimer.

residues in the bovine sequence that differ from the porcine or human sequences.

While some of the side-chain torsion angles of the T_6 bovine insulin structure vary from those of the porcine structure, functional groups such as amide or carboxyl groups are found to reside in the same relative areas. Apparent differences in torsion angles are therefore most likely a reflection of coordinate errors arising from the lower resolution of the present study.

3.2. Zinc coordination

Each zinc ion is octahedrally coordinated by three $N^{\varepsilon 2}$ atoms of three symmetry-related HisB10 residues and three symmetry-related water molecules. Zn—$N^{\varepsilon 2}$ distances are 2.06 and 2.10 Å, while Zn—OW distances are 2.31 and 2.41 Å for monomers 1 and 2, respectively. These values are comparable to those reported for T_6 porcine insulin (Baker *et al.*, 1988) of 2.05 and 2.05 Å for Zn—$N^{\varepsilon 2}$, and 2.36 and 2.21 Å for Zn—OW. Unlike the situation that is frequently observed in the T-state trimers in $T_3R_3^f$ hexamers (Ciszak & Smith, 1994), there was no evidence for tetrahedral or dual tetrahedral/octahedral coordination of the zinc ions.

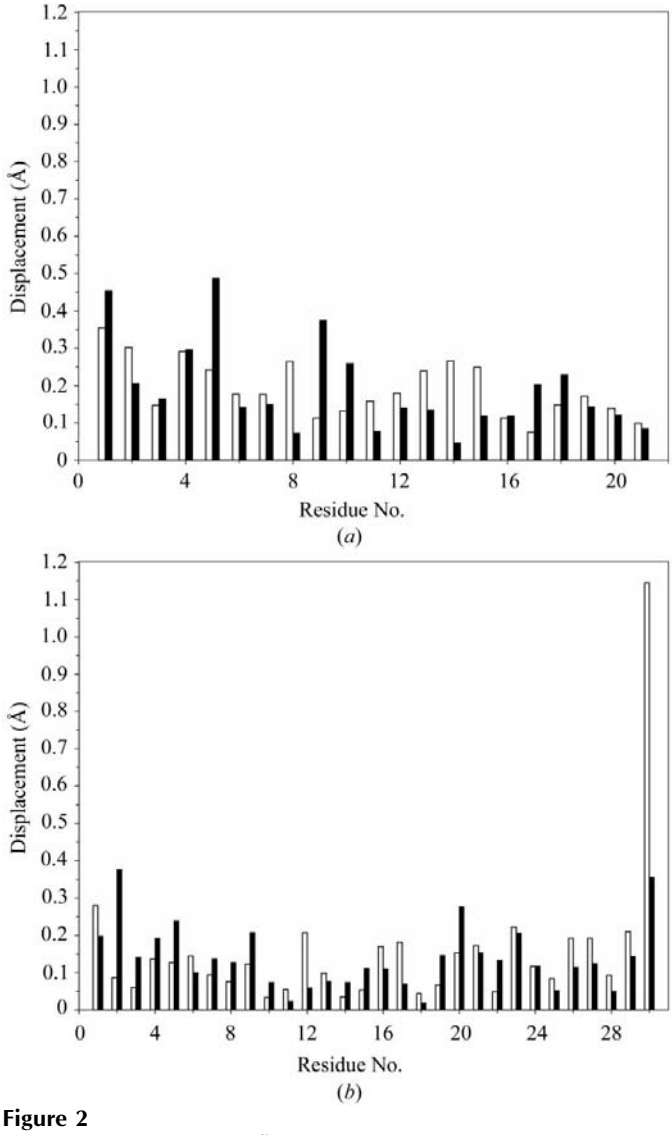

Figure 2
Histogram illustrating the C^{α} displacements of the (*a*) A chains and (*b*) B chains following the superposition of the dimer of the present study onto that of PDB entry 4ins. White bars refer to monomer 1; black bars refer to monomer 2.

3.3. GluB13 side chains and the central core water structure

In the T_6 porcine (Baker *et al.*, 1988) and human (Smith *et al.*, 2003) insulin hexamers, the side chains of GluB13 are directed towards the center of the hexamer, where very short contacts exist between $O^{\varepsilon 2}$ of GluB13.1 and $O^{\varepsilon 2}$ of GluB13.2. This same arrangement exists in the T_6 bovine hexamer with an O—O distance of 2.57 Å, illustrated in Fig. 3. While one would normally not expect the glutamate carboxyl groups to be protonated at a pH near 6.0, the pK_a of GluB13 has been reported to be larger than expected (Kaarsholm *et al.*, 1990) and is consistent with the interpretation of a centered carboxylate–carboxylic acid hydrogen bond (Smith *et al.*, 2003), also observed in the structure of $T_3R_3^f$ human insulin (Smith *et al.*, 2001).

In the 1.0 Å structure of T_6 human insulin, Smith *et al.* (2003) defined three threefold-symmetric layers of water in the central core of the hexamer. The first and third layers, related by a local twofold axis, contain a total of 26 water molecules. The second layer, situated between layers 1 and 3, contains three water molecules. Because of the poorer resolution and data quality in the present structure, it was not possible to observe one water molecule from layer 1 and seven water molecules from layer 3. In the higher resolution structure, the three waters in layer 2 are related by the crystallo-

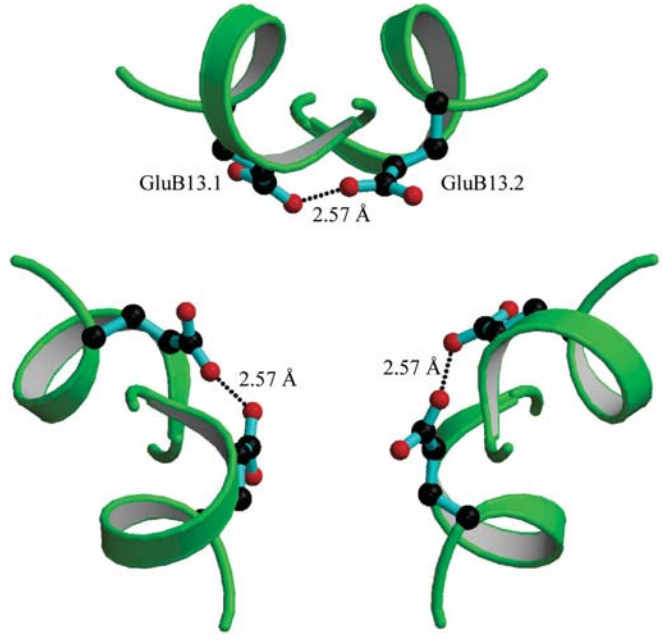

Figure 3
The GluB13 residues in the central core of the bovine insulin hexamer. The centered hydrogen bond is illustrated by the dotted line. This figure was prepared with the programs *MOLSCRIPT* (Kraulis, 1991) and *RASTER3D* (Merritt & Bacon, 1997).

Table 3
Hydrogen-bonded contacts involving water molecules in the central core of the T_6 bovine insulin hexamer.

Atoms		Distance (Å)	Symmetry
Layer 1			
603 O	HisB5.1 O	3.09	x, y, z
603 O	CysB7.1 N	2.89	x, y, z
629 O	SerB9.1 O^{γ}	2.59	x, y, z
629 O	GluB13.2 $O^{\varepsilon 2}$	2.71	x, y, z
633 O	GluB13.2 $O^{\varepsilon 1}$	2.80	x, y, z
633 O	645 O	2.47	$-x + y, -x, z$
645 O	HisB10.1 O	3.04	x, y, z
Layer 3			
606 O	GluB13.1 $O^{\varepsilon 2}$	2.50	x, y, z
606 O	SerB9.2 O^{γ}	2.49	x, y, z
628 O	GluB13.1 $O^{\varepsilon 1}$	3.15	$-x + y, -x, z$
628 O	HisB10.2 $N^{\delta 1}$	2.92	x, y, z

graphic threefold axis and form a hydrogen-bonded network amongst themselves. This trio of water molecules is replaced in the present structure by a single water molecule that resides on the crystallographic threefold axis. The mean displacement between the six independent water molecules in layers 1 and 3 and their counterparts in the T_6 human insulin hexamer is 0.47 (4) Å. Hydrogen-bonded contacts involving the waters in the central core in T_6 bovine insulin are listed in Table 3.

3.4. Structural consequences of the sequence change at A8 and A10

While there are numerous water-mediated hydrogen bonds between hexamers in the T_6 insulin structure, there are only five, five and seven independent hydrogen bonds (Table 4) between the respective bovine, porcine and human insulin hexamers and only two hydrogen-bonded contacts are common to all three structures (SerA9.1 O···HisB5.2 $N^{\varepsilon 2}$ and Asn18.1 $O^{\delta 1}$···ThrB27.2 $O^{\gamma 1}$). However, the five independent hydrogen-bonded contacts in bovine and porcine insulin are equivalent. Two of the hydrogen bonds that exist in T_6 human insulin but not in bovine or porcine insulin are a result of a conformational change at the N-terminus of the B chain of monomer 2 (7.9 Å displacement relative to the room-temperature structure), a result of cryocooling. Other differences in hydrogen-bonded contacts between human insulin and bovine or porcine insulin are a result of different side-chain conformations or a small displacement of the C-terminus of A21.2 in the human insulin structure.

The Matthews coefficient and solvent content (Matthews, 1968) were calculated to be 1.94 $Å^3\ Da^{-1}$ and 36.6%, respectively, for both porcine and bovine insulin. The contraction of the c axis by 0.24 Å in bovine insulin corresponds to a unit-cell volume decrease equivalent to the loss of 39 water molecules.

In bovine and porcine insulin, all interhexamer interactions involve contacts between monomer 1 and a symmetry-related monomer 2. These interactions can be divided into three categories based upon symmetry: two result from a translation of the hexamer along the c axis, while the third results from the action of a 3_2 axis. These interactions are shown schematically in Fig. 4 along with the three different symmetry elements. In one case, there is a single zone of residues (A8.1–A10.1) that form van der Waals contacts to symmetry-related residues B5.2 and A10.2 $(-y, x - y, z + 1)$.

In porcine insulin, the side chains of both ThrA8 residues make no direct contacts with a neighboring hexamer. Instead, $O^{\gamma 1}$ of ThrA8.1 forms a 2.39 Å hydrogen bond to a water molecule, which in turn forms a 3.02 Å hydrogen bond to a c-translationally related alternate side-chain conformation of

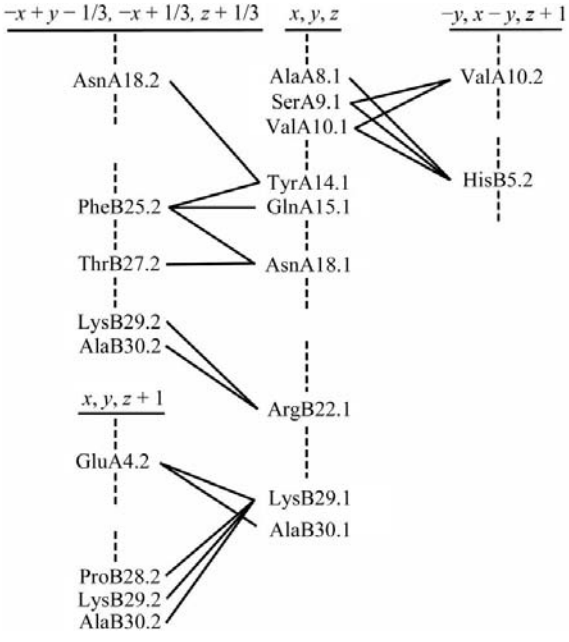

Figure 4
Schematic drawing illustrating the hydrogen-bonded and van der Waals contacts of less than 4.0 Å between bovine insulin hexamers. The symmetry elements that relate monomer 2 in the asymmetric unit to the three related monomers are underlined.

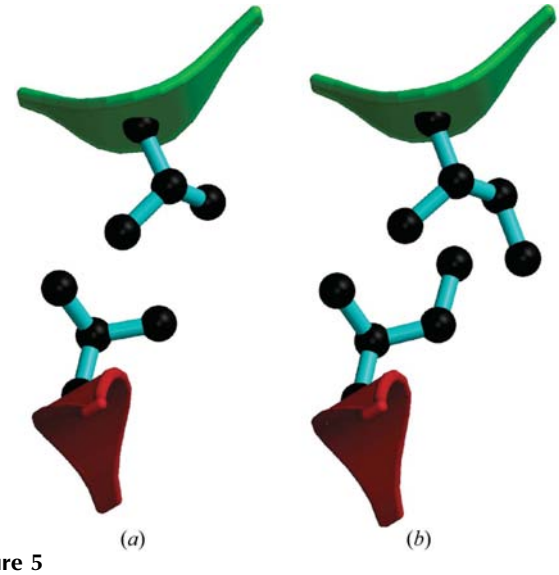

Figure 5
Interhexamer interactions between (*a*) the ValA10 side chains in bovine insulin and (*b*) the IleA10 side chains in porcine insulin. The backbone of A10.1 is colored green, A10.2 (related by $-y, x - y, z + 1$) is colored red and the side chains are colored cyan. This figure was prepared with the programs *MOLSCRIPT* (Kraulis, 1991) and *RASTER3D* (Merritt & Bacon, 1997).

Table 4
Interhexamer contacts of less than 3.4 Å in T_6 bovine, porcine and human insulin.

Hydrogen-bonded contacts are shown in bold.

Atoms		Distance (Å)				
		Bovine	Porcine	Human	Symmetry	
SerA9.1 O	HisB5.2 $N^{\varepsilon 2}$	**2.94**	**2.60**	**2.72**	$-y, x-y, z$	0, 0, 1
SerA9.1 O^{γ}	AsnB3.2 O	5.70	5.35	**2.74**	$-y, x-y, z$	0, 0, 1
LysB29.1 N^{ζ}	GluA4.2 $O^{\varepsilon 1}$	**2.79**	**3.05**	4.00	x, y, z	0, 0, 1
LysB29.1 N^{ζ}	AlaB30.2 O	**2.62**	**2.52**	3.23†	x, y, z	0, 0, 1
LysB29.1 N^{ζ}	AlaB30.2 OXT	4.15	3.59	3.14†	x, y, z	0, 0, 1
GlnA15.1 $N^{\varepsilon 2}$	AsnA21.2 $O^{\delta 1}$	4.06	4.11	**2.82**	$-x+y, -x, z$	−1/3, 1/3, 1/3
AsnA18.1 $O^{\delta 1}$	ThrB27.2 $O^{\gamma 1}$	**2.76**	**2.75**	**2.81**	$-x+y, -x, z$	−1/3, 1/3, 1/3
AsnA18.1 $O^{\delta 1}$	ThrB30.2 $O^{\gamma 1}$	†	†	**2.82**	$-x+y, -x, z$	−1/3, 1/3, 1/3
ArgB22.1 $N^{\eta 1}$	AlaB30.2 OXT	**3.19**	**2.91**	3.59†	$-x+y, -x, z$	−1/3, 1/3, 1/3
ThrB30.1 $O^{\gamma 1}$	PheB1.2 N	†	†	**2.90**	$-x+y, -x, z$	1/3, 2/3, 2/3

† In bovine, porcine and human insulin, the respective residues at B30 are alanine, alanine and threonine.

Table 5
Contacts of less than 4 Å between the A10 side chains in one hexamer and side-chain atoms in an adjacent hexamer related by $-y, x-y, z+1$.

The side chain of bovine Val A10.1 occupies two discrete positions: $C^{\gamma 1}$ and $C^{\gamma 2}$ of bovine ValA10.1 in the primary conformation correspond to H^{β} and $C^{\gamma 2}$ of porcine or human IleA10.1, respectively, while $C^{\gamma 1}$ and $C^{\gamma 2}$ of bovine ValA10.1 in the secondary conformation correspond to $C^{\gamma 2}$ and $C^{\gamma 1}$ of porcine or human IleA10.1, respectively.

Atoms		Bovine	Porcine	Human
ValA10.1 $C^{\gamma 2}$	ValA10.2 $C^{\gamma 1}$	3.87		
ValA10.1 $C^{\gamma 2}$	HisB5.2 $N^{\varepsilon 2}$	3.63		
ValA10.1 $C^{\gamma 1}$†	ValA10.2 $C^{\gamma 1}$	3.94		
IleA10.1 $C^{\gamma 2}$	IleA10.2 $C^{\gamma 2}$		4.22	4.14
ValA10.1 $C^{\gamma 1}$†	HisB5.2 $C^{\varepsilon 1}$	4.30		
IleA10.1 $C^{\gamma 2}$	HisB5.2 $C^{\varepsilon 1}$		4.01	3.82
ValA10.1 $C^{\gamma 1}$†	HisB5.2 $N^{\varepsilon 2}$	3.71		
IleA10.1 $C^{\gamma 2}$	HisB5.2 $N^{\varepsilon 2}$		3.95	3.86
ValA10.2 $C^{\gamma 1}$	SerA9.1 O^{γ}	3.86		
IleA10.2 $C^{\gamma 2}$	SerA9.1 O^{γ}		4.45	4.55
IleA10.2 $C^{\delta 1}$	SerA9.1 O^{γ}		3.67	3.36
IleA10.2 $C^{\delta 1}$	IleA10.1 $C^{\gamma 1}$		4.11	3.78
IleA10.2 $C^{\delta 1}$	IleA10.1 $C^{\delta 1}$		4.14	3.97

† Alternate side-chain conformation.

GluB21.1 $O^{\varepsilon 1}$. The 4.85 Å closest contact of the ThrA8.1 $C^{\gamma 2}$ is also to the disordered side chain of GluB21.1. Thus, the side chains of ThrA8.1 and ThrA8.2 make no contacts shorter than 6.0 Å to a neighboring hexamer. In bovine insulin there are no interhexamer protein–protein contacts shorter than 6.0 Å involving either of the AlaA8 residues. Since ThrA8.1 forms only a single water-mediated hydrogen bond between porcine insulin hexamers and involves a disordered side chain, this residue appears to have little or no effect upon the packing of the hexamers within the crystal.

The side chains of three symmetry-related A10.1 residues in one trimer lie on the surface of the hexamer in a plane perpendicular to the *c* axis, where they make van der Waals contacts with three A10.2 residues rotated by 120° and translated along the *c* axis. These interactions are illustrated in Figs. 5(*a*) and 5(*b*) for bovine and porcine insulin, respectively. Contacts of less than 4 Å involving the A10 side chains are listed in Table 5 for bovine, porcine and human insulin. Examination of this table shows that with one exception, the contacts observed between bovine insulin hexamers are shorter than those in either human or porcine insulin. Thus, the loss of the $C^{\delta 1}$ atom of human or porcine isoleucine A10 to produce bovine valine A10 results in shorter interhexamer contacts. This is also apparent from the 0.36 Å decrease in the distance between the C^{β} atoms of A10.1 and A10.2 in bovine and porcine insulin following the rotation and translation of A10.2 along the *c* axis. A comparison of the unit-cell parameters of porcine insulin to those of bovine insulin shows that the *c* dimension of T_6 bovine insulin has decreased by 0.24 Å, a direct consequence of the change in amino-acid sequence at A10 from isoleucine to valine. Thus, the net effect of the sequence change is to strengthen the stabilizing hydrophobic interactions between hexamers.

4. Conclusions

This study has shown that the conformations of bovine and porcine insulin are nearly identical, with r.m.s. deviations between the two dimers of 0.20 Å. Thus, the sequence differences at A8 and A10 produce no significant conformational perturbations in either the A-chain or B-chain conformations of bovine insulin relative to porcine or human insulin. However, the larger C^{α} displacements relative to T_6 porcine insulin observed for the first ten residues of both A chains do suggest that there is more conformational flexibility in this region than in other regions of the insulin monomer. A similar feature was noted for two dehydrated structures of T_6 human insulin (Smith & Blessing, 2003).

While the sequence change from threonine to alanine at A8 appears to have no effect upon the packing of the hexamers in the crystal, the change from isoleucine to valine at A10 does produce subtle differences in the packing. The loss of the $C^{\delta 1}$ methyl group of isoleucine allows a closer approach of the hexamers parallel to the *c* axis, as evidenced by the contraction of that unit-cell parameter in bovine insulin. This in turn reduces the distances between hydrophobic contacts in the hexamers and further stabilizes the packing of the hexamers in the crystal. While it is difficult if not impossible to accurately assess the effect of the change in the hydrophobic interactions upon dissolution rates of therapeutic insulin preparations, these results do suggest a role for the A10 residue in the superior pharmacodynamic profile of long-acting bovine insulin therapeutic preparations.

The authors wish to thank Dr Ronald E. Chance of Lilly Research Laboratories for a generous gift of highly purified

bovine insulin. This research was supported by NIH Grant GM56829.

References

Adams, P. D., Pannu, N. S., Read, R. J. & Brünger, A. T. (1997). *Proc. Natl Acad. Sci. USA*, **94**, 5018–5023.

Baker, E. N., Blundell, T. L., Cutfield, J. F., Cutfield, S. M., Dodson, E. J., Dodson, G. G., Hodgkin, D. C., Hubbard, R. E., Isaacs, N. W., Reynolds, C. D., Sakabe, K., Sakabe, N. & Vijayan, N. M. (1988). *Philos. Trans. R. Soc. London, Ser. B*, **319**, 369–456.

Blessing, R. H. (1997). *J. Appl. Cryst.* **30**, 421–426.

Bloom, C. R., Choi, W. E., Brzović, P. S., Huang, J. J., Kaarsholm, N. C. & Dunn, M. F. (1995). *J. Mol. Biol.* **245**, 324–330.

Brünger, A. T. (1992). *Nature (London)*, **355**, 472–474.

Brünger, A. T., Adams, P. D., Clore, G. M., DeLano, W. L., Gros, P., Grosse-Kunstleve, R. W., Jiang J., Kuszewski, J., Nilges, M., Pannu, N. S., Read, R. J., Rice, L. M., Simonson, T. & Warren, G. L. (1998). *Acta Cryst.* D**54**, 905–921.

Brünger, A. T., Adams, P. D. & Rice, L. M. (1997). *Structure*, **5**, 325–336.

Brzović, P. S., Choi, W. E., Borchardt, D., Kaarsholm, N. C. & Dunn, M. F. (1994). *Biochemistry*, **33**, 13057–13069.

Choi, W. E., Brader, M. L., Aguilar, V., Kaarsholm, N. C. & Dunn, M. F. (1993). *Biochemistry*, **32**, 11638–11645.

Ciszak, E., Beals, J. M., Frank, B. H., Baker, J. C., Carter, N. D. & Smith, G. D. (1995). *Structure*, **3**, 615–622.

Ciszak, E. & Smith, G. D. (1994). *Biochemistry*, **33**, 1512–1517.

Derewenda, U., Derewenda, Z., Dodson, E. J., Dodson, G. G., Reynolds, C., Sparks, K., Smith, G. D. & Swenson, D. C. (1989). *Nature (London)*, **338**, 594–596.

Graff, R. A. G. de, Lewit-Bentley, A. & Tolley, S. P. (1981). *Structural Studies on Molecules of Biological Interest*, edited by G. Dodson, J. P. Glusker & D. Sayre, pp. 547–556. Oxford: Clarendon Press.

Kaarsholm, N. C., Havelund, S. & Hougaard, P. (1990). *Arch. Biochem. Biophys.* **283**, 496–502.

Kaarsholm, N. C., Ko, H. & Dunn, M. F. (1989). *Biochemistry*, **28**, 4427–4435.

Kraulis, P. (1991). *J. Appl. Cryst.* **24**, 946–950.

Krüger, P., Gilge, G., Çabuk, Y. & Wollmer, A. (1990). *Biol. Chem. Hoppe-Seyler*, **137**, 669–673.

Laskowski, R. A., MacArthur, M. W., Moss, D. S. & Thornton, J. M. (1993). *J. Appl. Cryst.* **26**, 283–291.

Matthews, B. W. (1968). *J. Mol. Biol.* **33**, 491–497.

Merritt, E. A. & Bacon, D. J. (1997). *Methods Enzymol.* **277**, 505–524.

Otwinowski, Z. & Minor, W. (1997). *Methods Enzymol.* **276**, 307–326.

Pannu, N. S. & Read, R. J. (1996). *Acta Cryst.* A**52**, 659–668.

Read, R. J. (1986). *Acta Cryst.* A**42**, 140–149.

Rice, L. M. & Brünger, A. T. (1994). *Proteins*, **19**, 277–290.

Richards, J. P., Stickelmeyer, M. P., Frank, B. H., Pyle, S., Barbeau, M., Radziuk, J., Smith, G. D. & DeFelippis, M. R. (1999). *J. Pharm. Sci.* **9**, 861–867.

Sack, J. S. (1988). *J. Mol. Graph.* **6**, 244–245.

Seigler, D. E., Olsson, G. M., Agramonte, R. F., Lohman, V. L., Ashby, M. H., Reeves, M. L. & Skyler, J. S. (1991). *Diabetes Nutr. Metab.* **4**, 267–273.

Smith, G. D. (1993). *PROFIT. A Locally Written Program for Orienting One Protein Molecule Onto Another by a Least-Squares Procedure.* Hauptman–Woodward Medical Research Institute, Buffalo, USA.

Smith, G. D. & Blessing, R. H. (2003). *Acta Cryst.* D**59**, 1384–1394.

Smith, G. D., Ciszak, E., Magrum, L. A., Pangborn, W. A. & Blessing, R. H. (2000). *Acta Cryst.* D**56**, 1541–1548.

Smith, G. D., Ciszak, E. & Pangborn, W. A. (1996). *Protein Sci.* **5**, 1502–1511.

Smith, G. D. & Dodson, G. G. (1992). *Proteins*, **14**, 401–408.

Smith, G. D., Pangborn, W. A. & Blessing, R. H. (2001). *Acta Cryst.* D**57**, 1091–1100.

Smith, G. D., Pangborn, W. A. & Blessing, R. H. (2003). *Acta Cryst.* D**59**, 474–482.

Smith, G. D., Swenson, D. C., Dodson, E. J., Dodson, G. G. & Reynolds, C. D. (1984). *Proc. Natl Acad. Sci. USA*, **81**, 7093–7097.

Whittingham, J. L., Chaudhurri, S., Dodson, E. J., Moody, P. C. E. & Dodson, G. G. (1995). *Biochemistry*, **34**, 15553–15563.